Single Cell RNA-Sequencing-based Analysis of CD4$^+$ T-Cell Subset-Specific Susceptibility to Transcriptional Modulation by HIV-1 Latency-Reversing Agents

Julia Kazmierski[1,2], Dylan Postmus[1,2], Emanuel Wyler[3], Cornelius Fischer[4], Jenny Jansen[1,2], Karolin Meixenberger[5], Sarah Nathalie Vitcetz[4], Madlen Sohn[4], Sascha Sauer[4], Norbert Bannert[1,5], Markus Landthaler[3,6], and Christine Goffinet[1,2*]

[1]Institute of Virology, Campus Charité Mitte, Charité - Universitätsmedizin Berlin, Charitéplatz 1, 10117 Berlin, Germany

[2]Berlin Institute of Health, 10178 Berlin, Germany

[3]Berlin Institute for Medical Systems Biology, Max-Delbrück-Center for Molecular Medicine in the Helmholtz Association, Robert-Rössle-Strasse 10, 13125 Berlin, Germany

[4]Scientific Genomics Platforms, Laboratory of Functional Genomics, Nutrigenomics and Systems Biology, Max Delbrück Center for Molecular Medicine, 13125 Berlin, Germany.

[5]Division of HIV and Other Retroviruses, Robert Koch Institute, Berlin, Germany

[6]IRI Life Sciences, Institute für Biologie, Humboldt Universität zu Berlin, Philippstraße 13, 10115 Berlin, Germany

*Corresponding author:

Christine Goffinet, Institute of Virology, Campus Charité Mitte, Charité - Universitätsmedizin Berlin, Charitéplatz 1, 10117 Berlin, Germany

Phone: +0049 30 450 525 489

e-mail: christine.goffinet@charite.de

Keywords: HIV-1, latency-reversing agents, $CD4^+$ T-cells, interferon, interferon-regulated genes, single cell-RNA sequencing

Abstract

Shock-and-kill is one of the conceptually most advanced strategy towards establishment of an HIV-1 cure. Treatment with latency-reversing agents (LRAs), including histone deacetylase inhibitors with chromatin-remodeling capabilities, combined with anti-retroviral therapy, reactivates HIV-1 transcription *in vivo*. However, LRA treatment fails to significantly reduce the HIV-1 reservoir in HIV-1-positive individuals, indicating that it is probably insufficient to eliminate latently infected cells. The global and T-cell subset-specific impact of individual LRAs on the transcriptome of $CD4^+$ T-cells, the main HIV-1 reservoir containing cell type *in vivo*, remains understudied. Here, using single cell RNA-sequencing, we characterize LRA treatment-induced alterations of $CD4^+$ T-cell subset composition and of subpopulation-specific transcriptomes, using Vorinostat and Panobinostat as two prototypic HDAC inhibitors. *Ex vivo* exposure of $CD4^+$ T-cells from an aviremic HIV-1-positive individual to Panobinostat markedly reduced the percentage of T_{REG} cells. Furthermore, it altered expression of a multitude of interferon-regulated genes, resulting in suppression of several well-characterized antiviral genes, and in enhancement of selected interferon-regulated genes with proviral activities. These changes were most pronounced in T_N, T_{CM}, T_{TM} and T_{EM}, and less pronounced in T_{REG}. Exposure to Vorinostat resulted in a comparably mild change of cellular transcriptomic profile, regarding both the number of deregulated genes and their fold change of expression. Nevertheless, selected interferon-regulated genes exhibited a subset-specific expression profile upon Vorinostat treatment. Finally, some genes were deregulated by both treatments in a subset-specific manner. We conclude that treatment by both individual HDAC inhibitors induces an overall proviral milieu in $CD4^+$ T-cells subsets. While this proviral state might be favorable for efficient HIV-1 reactivation, we hypothesize that it may impede the instruction of activation of cellular and adaptive immunity required for effective killing of reactivated cells.

Introduction

The development and implementation of highly active antiretroviral therapy (HAART) is established as an effective tool for suppressing viremia and improving the quality and duration of life for individuals living with HIV/AIDS. However, though these patients may exhibit undetectable plasma levels of the virus during optimal treatment, latently infected cells persist and expand (Vanhamel et al., 2019). In addition, cessation of treatment ultimately results in a return to a viraemic state within weeks in the vast majority of HIV-1-positive individuals (Hurst et al., 2015).

The HIV-1 reservoir is maintained by long-lived, latently infected $CD4^+$ T-cells and cells from the monocyte/macrophage lineage. Among resting $CD4^+$ T-cells carrying latent HIV-1, T_{CM} and T_{TM} predominate, but latent HIV-1 also resides in T_N and T_{EM} , albeit to a lower percentage (Chomont et al., 2009). The viral reservoir displays a very long half-life and slow decay rate, with predicted 73 years of antiretroviral therapy that would be required for eradication (Finzi et al., 1999; Siliciano et al., 2003). A main mechanism of persistence of the viral reservoir during antiretroviral treatment is clonal expansion through homeostatic proliferation, as indicated by a vast majority of $CD4^+$ T-cells in treated patients sharing identical HIV-1 genome sequence and integration site (Cohn et al., 2015; von Stockenstrom et al., 2015; Wagner et al., 2014) or TCR sequence (Cohn et al., 2018). Of recent interest as a potential cure strategy is the so-named shock-and-kill approach. It is based on the administration of latency-reversing agents (LRAs), including histone deacetylase (HDAC) inhibitors, combined with antiretroviral treatment, and is anticipated to reactivate viral transcription in these reservoirs and thus target virus-infected cells for eradication by immunological or pharmacological means (Kim et al., 2018; Margolis et al., 2016). Clinical trials addressing the ability of individual LRAs to purge latent HIV-1 *in vivo* demonstrated reactivation of latent HIV-1 but no detectable reduction of the viral reservoir (Archin et al., 2012; Rasmussen et al., 2014; Sogaard et al.,

2015). It has been suggested that individual LRAs display distinct specificities and potencies with regards to different T-cell sub-populations (Grau-Exposito et al., 2019), resulting in suboptimal responses in some, but not other subsets. Furthermore, PHA-reactivated $CD4^+$ T-cells have been reported to display differential expression of genes related to cellular antiviral immunity (Cohn et al., 2018). Here, we exposed $CD4^+$ T-cells isolated from an aviremic HIV-1-positive individual to Vorinostat and Panobinostat, respectively, and investigated, in individual T-cell subsets and by single cell RNA-sequencing, LRA-specific global transcriptomic changes and modulation of expression of cellular genes implicated in cell-intrinsic innate immunity.

Methods & Materials

$CD4^+$ T-Cells from an Aviremic HIV-1 Patient

EDTA blood was collected in the context of the German HIV-1 Seroconverter Study (Machnowska et al., 2019) with approval of the local ethics committee (Ethical review committee of Charité University Medicine Berlin, Germany, EA 2/105/05). All study patients sign an informed consent form prior to enrollment. $CD4^+$ T-cells were isolated using the EasySep Direct Human $CD4^+$ T Cell Isolation Kit (STEMCELL Technologies). Cells were cultured at 2×10^6/ml in RPMI 1640 containing 10% heat-inactivated fetal calf serum (Sigma-Aldrich), 1% penicillin-streptomyin (Thermo Fisher Scientific), 2 mM L-glutamine (Thermo Fisher Scientific), 1x MEM Non-essential Amino Acid Solution (Thermo Fisher Scientific) and 1mM Sodium Pyruvate (Thermo Fisher Scientific).

Reagents

IL-2 and PHA were purchased from Roche and Oxoid, respectively. Panobinostat was obtained from Cayman Chem. Vorinostat was obtained through the NIH AIDS Research & Reference Reagent Program.

IL-2/PHA Stimulation and Treatment with Latency-Reversing Agents

$CD4^+$ T-cells were mock-treated or treated individually with Vorinostat (500 nM), Panobinostat (50 nM) or IL-2 (20 U/ml)/PHA (1 µg/ml) for 48 hours.

Single cell RNA sequencing

Single Cell RNA-Seq libraries were prepared with the 10x Genomics platform using the Chromium Next GEM Single Cell 3' Reagent Kits v.3.1 following manufacturer's instructions. Quality control of the libraries was performed with the KAPA Library Quantification Kit (KK4854, Roche) and Agilent TapeStation (5067-5584, Agilent). Libraries were sequenced on a HiSeq 4000 (Illumina) device using the following sequencing mode: read 1: 28 bp, read 2: 91-100 bp, Index i7: 8 bp. The libraries were sequenced to reach ~20 000 reads per cell.

Data Presentation and Statistical Analysis

Cell clustering, cell subset type identification and differential expression analysis

Analysis of the scRNA data was performed using R Studio v3.6 (R Core Team, 2017) and the Seurat v3.1.4 package (Butler et al., 2018). Filtered Cell Ranger (v 3.1.0) matrices were imported into R and analysed according to the guidelines set out by the Satija Lab website. The data were initially filtered to remove cells with fewer than 500 unique detected genes to ensure adequate sequencing depth, as well as cells with unusually high numbers of gene reads, which likely represent cell multiplets, and cells with more than 10% mitochondrial DNA reads, as

these represent dead cells. After filtration, a total of 22715 cells remained. The data was log-normalised and scaled using the LogNormalize and ScaleData functions. Principal component analysis and linear dimensional reduction analysis using a Uniform Manifold Approximation and Projection (UMAP) plot were performed, where cells were clustered by means of a Shared Nearest Neighbor (SNN) graph, based on a K-Nearest Neighbor graph. In general, a resolution parameter of 1.0 or higher was used to cluster cells in order to retrieve a maximum amount of clusters. Identities of clusters were determined using a graph-based clustering approach and the list of pre-determined cell marker genes. Integration of datasets was performed using Seurat's in-built toolset for finding 'anchors' between datasets (FindIntegrationAnchors) via a canonical correspondence analysis (CCA). Testing for differential gene expression was performed using a Wilcoxon sum rank test with a Bonferroni correction. Only genes with a natural log fold-change of at least ±0.25 (1.28 or 0.77 fold change) and that were expressed in at least 10% of cells in either the mock treated or LRA-treated sample were included, where an adjusted p-value of lower than 0.05 was considered significant. As the analysis focussed on $CD4^{+}$ T cells, any clusters identified as $CD8^{+}$ cells, NK cells ($CD3D^{-}$, $NKG7^{hi}$, $GNLY^{hi}$) or dead cells (where the most significantly differentially regulated genes were mitochondrial in origin) were manually removed.

Cell trajectory and GSEA analysis

Cell trajectory/Pseudotime analysis was performed using the Monocle v2.14.0 package (Trapnell et al., 2014) according to the guidelines on the Monocle website. Data from the created Seurat object was imported into Monocle as raw counts (UMI). For each cell subset, genes identified to be significantly differentially regulated based on the above-mentioned criteria were used as the ordering genes for the Pseudotime analysis. The minimum spanning tree was generated using the DDRTree algorithm and the cells arranged along the resulting Pseudotime trajectory. This was also performed using all genes differentially expressed

between treated and mock-treated cells across all cell subsets. As very few (<10) Treg cells in the Panobinostat treatment could be identified, these were omitted from the trajectory analysis. Genes defining the branchpoint observed in the trajectory analysis were determined using a branch expression analysis model (BEAM). Gene set enrichment analysis (GSEA) was performed on the same genes used for ordering in the trajectory analysis using the fGSEA v1.12.0 package for R (Korotkevich et al., 2019). The analysis was performed using 10000 permutations, with the REACTOME curated pathway dataset (Jassal et al., 2020) obtained from the MSigDB R package (msigdbr) v7.0.1 used as the input pathway list. Of the full lists of differentially regulated genes for each cell subset and treatment, genes that represented interferon-regulated genes (IRGs) were identified by cross-referencing these lists with the Interferome 2.01 database (Rusinova et al., 2013). Differential expression testing was then performed as described.

Additional data visualisation

Venn diagrams depicting the intersection of genes differentially expressed amongst different cell types were generated using the venn R package v1.9 (Dusa, 2020), while those depicting the intersection in different LRA treatments were generated using the VennDiagram R package v1.6.20 (Chen, 2018). Heatmaps were generated using GraphPad Prism (Version 8.3.0). All other plots were generated using the ggplot2 R package (Wickham, 2016).

Results

In order to characterize LRA-specific effects and $CD4^+$ T-cell subpopulation-specific susceptibilities to individual LRAs, we exposed purified $CD4^+$ T-cells isolated from an aviremic, HIV-1 positive individual (Table S1) to Vorinostat, Panobinostat, IL-2/PHA or left them mock-treated for 48 hours, and subjected them to single cell RNA-sequencing. We chose to test Vorinostat and Panobinostat due to their demonstrated efficacy to reactivate HIV-1 mRNA expression *in vivo* (Archin et al., 2012; Rasmussen et al., 2014). The employed concentrations and duration of Vorinostat and Panobinostat treatment correspond to the documented ability of the drugs to reactivated HIV-1 *in vitro* (Rasmussen et al., 2013; Tsai et al., 2016). We included IL-2/PHA treatment as a reference that we expected to result in maximum and relatively unspecific activation of T-cells. Finally, we decided to restrict our study on $CD4^+$ T-cells from an aviremic HIV-1-positive individual, as opposed to T-cells from a healthy individual for two reasons. First, this strategy allowed us to consider potential changes of the T-cell composition and transcriptome in the context of a preceding HIV-1 infection and long-term antiretroviral treatment (Wang et al., 2019). Second, we aim to correlate, at the single cell level, identified transcriptomic signatures to patterns and efficiencies of HIV-1 mRNA expression.

We used a graph-based clustering approach and T-cell subset-specific marker genes to assign cells into different subsets (Fig. 1A-C). The cells were grouped into naive $CD4^+$ T-cells (T_N; $CD8A^-$, $CD3D^+$, $CCR7^+$, $IL7R^{hi}$), central memory $CD4^+$ T-cells (T_{CM}; $CD8A^-$, $CD3D^+$, $CCR7^+$, $S100A4^{int}$, $IL7R^+$, $SELL^{hi}$) (Golubovskaya and Wu, 2016; MacLeod et al., 2009), transitional memory T-cells (T_{TM}; $CD8A^-$, $CD3D^+$, $CCR7^{lo}$, $IL7R^+$, $S100A4^{hi}$, $SELL^{lo}$, $GZMA^-$, $CD27^+$) (Mahnke et al., 2013), effector memory $CD4^+$ T-cells (T_{EM}; $CD8A^-$, $CD3D^+$, $CCR7^-$, $IL7R^+$, $S100A4^{hi}$, $CD27^-$, $GZMA^+$) (Golubovskaya and Wu, 2016; Weatherly et al., 2015), $CD4^+$ regulatory T-cells (T_{REG}; $CD8A^-$, $CD3D^+$, $FOXP3^+$, $IL2RA^+$) (Golubovskaya and Wu,

2016) and a subset we defined as effector lo $CD4^+$ T-cells ($CD8A^-$, $CD3D^+$, $CCR7^-$, $IL7R^+$, $S100A4^{hi}$, $CD27^-$, $GZMA^{lo}$), which defined a separate cluster expressing low levels of GZMA but relatively high levels of other effector molecules (GNLY, GZMB).

While exposure to Vorinostat did not grossly alter the $CD4^+$ T-cell subtype composition, individual treatment with Panobinostat and IL-2/PHA substantially altered relative percentages of $CD4^+$ T-cell subsets (Fig. 1B-C). Panobinostat treatment induced an almost entire eclipse of T_{REG} cells (0.1%, versus 6% in mock-treated cells). Furthermore, it enlarged the pool of T_N cells (38.4% versus 26.2% in mock-treated cells). IL-2/PHA treatment resulted in appearance of a separate cluster of cells we referred to as effector lo $CD4^+$ T_{EM}-cells. We hypothesize that this additional cell cluster represents a transitory state of differentiation between T_{TM} and T_{EM}-cells, which would be in line with the canonical role of IL- 2 as an inducer of T-cell differentiation towards effector memory status (Ross and Cantrell, 2018) (Figure 1A-C).

LRA- and $CD4^+$ T-cell subset specific modulation of the transcriptome

Integrated analysis of the composition of $CD4^+$ T-cells in the absence and presence of a specific treatment revealed a noticeably altered topography of the UMAP in the case of treatment with Panobinostat and IL-2/PHA relative to Vorinostat. Indeed, though Seurat's toolkit for integrated analysis is robust in promoting cell subset-specific clustering despite treatment-specific effects, we observed the emergence of several clusters comprising almost entirely of cells from the LRA treatment (T_N cells in the case of Panobinostat, as well as T_N, T_{CM} and T_{TM} cells in the case of IL2-PHA treatment). Though this observation alone is insufficient to make a solid conclusion about gene expression profiles, it is in agreement with our observations that the transcriptomes of Panobinostat and IL-2/PHA treated cells appear to be radically altered in comparison to the Vorinostat treatment (Fig. 2A).

The number of statistically significantly ($p < 0.05$, $0.78 \leq$fold-change ≥ 1.28) deregulated genes varied between individual treatments and among $CD4^+$ T-cell subsets. Exposure to

Vorinostat induced deregulation of relatively few genes in all five subpopulations (Fig. 2B, Table S2). Panobinostat treatment resulted in altered expression of several hundred genes in most $CD4^+$ T-cell subsets, except T_{REG} $CD4^+$ T-cells, which presented a lower degree of responsiveness to this HDAC inhibitor treatment compared to the other subsets. IL-2/PHA treatment changed the transcriptome in all five sub-populations (Fig. 2B). In all $CD4^+$ T-cell subsets except T_{REG}, most genes deregulated by Vorinostat were also modulated by the two other treatments (Fig. 2C).

The relatively few genes modulated by Vorinostat were evenly distributed among the $CD4^+$ T-cell sub-populations, with T_{REG} presenting the highest number of unique differentially expressed genes (DEGs) (29 DEGs), and T_{TM} displaying not a single specific DEG (Fig. 2D). All individual T-cell subsets expressed a relatively unique set of 43-170 different genes in the context of treatment with Panobinostat, and presented some overlap between T_N and T_{CM} (85 DEGs), T_{TM} and T_{EM} (43 DEGs), and T_{TM} and T_{CM} (51 DEGs), indicating that treatment induces a T-cell subset-specific transcriptomic change (Fig. 2D). All subsets excluding T_{REG} shared 593 DEGs upon Panobinostat treatment. IL-2/PHA treatment induced a large number of DEGs in all subsets, 876 deregulated in all five sub-populations (Fig. 2D).

In order to investigate whether the altered gene expression profile in the Panobinostat treated sample induced a single or multiple cell trajectories and which pathways were most associated with this profile at cell subset level, we performed Pseudotime and gene set enrichment analysis (GSEA). Genes significantly differentially regulated in the treated versus mock cells for each subset were used as ordering and input genes, respectively. As there were very few T_{REG} cells in the Panobinostat treated sample, this cell subset was omitted from the analysis as we concluded that the results would likely not be conclusive (Fig. 2E). Cell trajectory analysis revealed that for all of the subsets, except T_N cells, the altered gene expression profile defines a single cell fate. For T_N cells, branched expression analysis modeling (BEAM) revealed that the differentially expressed genes defining the branchpoint are

comprised largely of genes encoding ribosomal structural proteins (Supplementary Figure S1). Interestingly, the positively and negatively enriched pathways in all subsets were similar (Fig. 2F). Generally, positively enriched pathways related to either cell stress, as in the DNA repair, cellular response to stress and cellular senescence pathways, or to cell proliferation and productivity, as in the case of the cilium assembly, nonsense mediated decay (NMD), rRNA processing and organelle biogenesis and maintenance pathways (Han et al., 2018; Sanchez and Dynlacht, 2016). In contrast, the negatively enriched pathways relate largely to immune function, such as the TCR signaling, adaptive immune signaling, cytokine immune signaling and immunoregulatory interactions between a lymphoid and non-lymphoid cell, suggesting that Panobinostat-treated cells may exhibit an impaired immune response capability. This migration of cells towards a single cell fate defined by Panobinostat treatment was recapitulated in the Pseudotime analysis combining all $CD4^+$ T-cell subsets. Interestingly, as the path through Pseudotime is followed, the root state (containing largely T_N cells) branches off into two cell fates – a branch containing entirely mock treated cells with a high representation of T_{EM} cells and a branch containing all of the Panobinostat treated cells. This branching implies that the trajectory of T_{EM} cells is largely contrarian to the transcriptomic profile induced by treatment, which is in line with the observation that Panobinostat appears to downregulate immune response pathways. Simultaneously, despite some cells having a very different transcriptomic profile to begin with, it becomes clear that Panobinostat induces a single and similar cell fate across all cell subsets.

LRA treatment alters the expression of IRGs in $CD4^+$ T-cells in a treatment- and subset-specific manner

In order to better understand how LRA treatment modulates the landscape of interferon-regulated genes (IRGs), we determined the fraction of all DEGs representing IRGs according to and using Interferome v2.01 (Rusinova et al., 2013). Interestingly, the majority of DEGs

represented IRGs (80%, 68%, 46% for Vorinostat, Panobinostat and IL-2/PHA, respectively). Consequently, due to the overall higher degree of gene expression alteration, treatment with IL-2/PHA and Panobinostat led to a much broader panel of differentially expressed IRGs than did treatment with Vorinostat (Fig. 3A). While Vorinostat treatment tended to result in a balanced number of up- and downregulated IRGs, Panobinostat treatment provoked more than twice the number of downregulated versus upregulated IRGs in T_{CM}, T_{TM} and T_{EM} cells. IL-2/PHA, in contrast, consistently resulted in a considerably larger ratio (generally at least two- to three-fold) of upregulated, compared to downregulated, IRGs (Figure 3A).

While Vorinostat treatment resulted in 75 differentially regulated IRGs across all $CD4^+$ T-cell subsets, individual exposure to Panobinostat and IL-2/PHA resulted in 1139 and 1342 differentially expressed IRGs, respectively. Of these, only 5, 29 and 509 for the Vorinostat, Panobinostat and IL-2/PHA exposure, respectively, were identified as differentially regulated across all T-cell sub-populations within the individual treatments (Fig. 3B), implying that alterations in the cellular IRG expression profile are predominantly subset-specific for all LRAs. Furthermore, the altered IRG profile observed in each cell subtype was largely determined by the specific LRA. Generally, while there was a sizeable overlap in IRGs differentially regulated by both Panobinostat and IL-2/PHA, we observed a substantial number of IRGs whose expression was only affected by treatment with either Panobinostat or IL-2/PHA. For example, in T_N cells, only 18 IRGs are differentially expressed upon all three individual treatments, while 412 IRGs were affected by Panobinostat and Il-2/PHA but Vorinostat and a further 363 and 891 genes were uniquely affected by Panobinostat and IL-2/PHA, respectively (Figure 3C).

In the context of Vorinostat and Panobinostat treatment, we focused our attention on significantly deregulated IRGs whose gene products have been characterized to serve as antiviral restriction factors, to be implicated in downstream signaling upon PRR triggering through viral PAMPs, and to be otherwise implicated in HIV-1 biology. Strikingly, analysis of

their expression level upon treatment (in comparison to mock treatment), revealed a marked downregulation in most, but not all subsets. Importantly, some key anti-HIV-1 factors, such as *APOBEC3G* (Sheehy et al., 2002), *IFITM1*-3 (Compton et al., 2014; Foster et al., 2016; Tartour et al., 2014), *MX2* (Goujon et al., 2013; Kane et al., 2013; Liu et al., 2013) and *SAMHD1* (Hrecka et al., 2011; Laguette et al., 2011) were downregulated in the context of Panobinostat treatment for the majority of cell subsets. *GBP5*, a gene encoding a cellular factor that interferes with HIV-1 Env processing and maturation (Braun et al., 2019; Krapp et al., 2016) displayed a subset-specific regulation of expression, with most pronounced downregulation in T_{REG}, weak downregulation in T_N and T_{TM}, virtually no alteration in T_{CM} and upregulation in T_{EM}. Interesting exceptions to this trend were *CDC37* and *HSP90AB1*, whose gene products act in complex on regulation of HIV-1 latency (Anderson et al., 2014) and *LGALS1*, an IRG encoding a protein facilitating HIV-1 attachment to target cells (Mercier et al., 2008; Ouellet et al., 2005; St-Pierre et al., 2011). The latter and all three factors were markedly upregulated by Vorinostat and Panobinostat, respectively, in most T-cell subsets (Fig. 3D-E). Importantly, some key antiviral factors, such as *TRIM56* (Kane et al., 2016 PMID 27631702), *SUN2* (Donahue *et al*., 2016 PMID: 26865710 SUN2) and *IFITM1*-3 (Tartour et al., 2014 PMID 25422070; Foster et al., 2016; Compton et al., 2014 PMID:25464829) were downregulated by Panobinostat treatment for the majority of cell subsets (Figure 3D-E). Taken together, these data imply that Vorinostat and Panobinostat treatments may result in an abrogated innate immune response and potentially a more proviral milieu in $CD4^+$ T-cells.

Discussion

The eminent aim of a LRA treatment in the context of HIV-1 cure is reactivation of HIV-1 mRNA and protein expression. This is supposed to occur through relatively unspecific remodulation of cellular chromatin by currently tested LRAs, boosting transcriptional reactivation of latent HIV-1 genomes but concomitantly resulting in expression changes of a multitude of cellular genes. How those transcriptomic changes of cellular genes indirectly impact HIV-1 reactivation and susceptibility of cells to re-infection remains understudied. An optimal shock-and-kill regimen must be, on the one hand, proviral with regards to all post-integrational steps. It should support or even boost Tat-mediated trans-activation of transcription, protein expression, and cellular trafficking of viral proteins in order to turn previously latent cells in immunologically visible cells which display Env and MHC-presented viral epitopes at the surface. On the other hand, an optimal shock-and-kill strategy must also trigger antiviral immune mechanisms, including cell-mediated immunity by CD8- and NK-cell-mediated cytotoxicity. Along this line, it has been suggested that a reduction of HIV-1 DNA levels during latency reversal is associated with distinct patterns of ISG expression (Olesen et al., 2015). HDAC inhibitors have clearly demonstrated their ability to promote reactivation of HIV-1 mRNA synthesis and protein expression *in vivo* and *in vitro* (Archin et al., 2012; Rasmussen et al., 2013; Rasmussen et al., 2014; Sogaard et al., 2015; Tsai et al., 2016). In *ex vivo*-treated $CD4^+$ T-cells, Vorinostat, Panobinostat and Romidepsin enhanced HIV-1 *de novo* infection (Lucera et al., 2014), raising concerns on potential spread of HIV-1 during shock-and-kill regime in body compartments insufficiently targeted by HAART. On the contrary, another report presented rather an antiviral and no effect of Romidepsin and Panobinostat, respectively (Jonsson et al., 2015). In addition to the missing or controversial knowledge on the net cellular state that is overall induced in LRA-treated $CD4^+$ T-cell cultures, there is no information on subset-specific impact of individual LRAs, and also not if, within a given T-cell subset, there are individual susceptibilities to LRA treatment at the single cell level. Given the preferential

occurrence of latent HIV-1 in T_{CM} and T_{TM}, and potential subtle particularities of cells harboring latent HIV-1 DNA as opposed to their HIV-1 negative counterparts, the characterization of the susceptibility to LRA treatment at the greatest possible level of detail is urgently required.

Vorinostat induced rather subtle changes in the $CD4^+$ T-cell subset composition and in the cellular transcriptome of individual T-cell subpopulations. A previous report using a higher concentration and shorter treatment duration suggested that genes promoting and inhibiting HIV-1 transcription were both upregulated in Vorinostat-treated $CD4^+$ T-cells (Beliakova-Bethell et al., 2019). Based on the current status of our analyses, we observe that several IRGs with documented anti-HIV-1 activity are downregulated in most T-cell subsets, and one interferon-modulated gene with a proviral function (*LGALS1*) is upregulated. Based on these observations, Vorinostat seems to promote an overall rather proviral state. Interestingly, not all subtypes were equally susceptible to this pattern, pointing to the idea that T_{EM} may be slightly more resistant to the Vorinostat-mediated suppression of antiviral IRGs. Future studies are required to identify if this correlates to a less efficient reactivation of latent HIV-1 in this particular $CD4^+$ T-cell subtype. Interestingly, Vorinostat has been reported to reactivate endogenous retroviruses (White et al., 2018), and investigation of this issue in our dataset is imminent.

Exposure of $CD4^+$ T-cells to Panobinostat for 48 hours resulted in an almost entire disappearance of T_{REG} cells. This finding appears to contradict results obtained upon *in vivo* administration of Panobinostat to HIV-1 patients in the context clinical latency reversal trials, which demonstrated a profound and reversible expansion of T_{REG} cells (Brinkmann et al., 2018). One possibility to reconcile those findings is that Panobinostat´s effect may not be restricted to $CD4^+$ T-cells *in vivo* and may have triggered expansion of T_{REG} via indirect effects, involving other cell types than $CD4^+$ T-cells. Importantly, another study suggested that Panobinostat treatment *in vitro*, and in the context of co-administration with the cytidine analog azacitidine

in vivo, lowered the frequency of a specific T_{REG} subset that is elevated in frequency in the peripheral blood of acute myeloid leukemia patients (Govindaraj et al., 2014).

Panobinostat treatment clearly modulated the transcriptional landscape of all $CD4^+$ subsets. We currently cannot exclude that the apparently smaller pool of deregulated genes in T_{REG} may be related to the reduction of frequency of this subset itself. Nevertheless, the other four T-cell subsets generally shared the downregulation of IRGs with antiviral activity, with some notable exceptions for individual genes in individual subsets. We are currently analyzing the T-cell subpopulation-specific expression pattern for HIV-1 latency modulating genes.

The preliminary findings of this study must be interpreted with caution. They are based on findings obtained from cells from a single donor, and currently performed analyses on cells from additional donors will be included very soon. Furthermore, the correlation analysis of the identified, partially subtype-specific cellular transcriptomic patterns to HIV-1 mRNA expression is an important ongoing task. Interestingly, preliminary experiments indicate that despite the limited number of cells analyzed, and despite the relative rarity of HIV-1-positive cells in the peripheral blood of aviremic individuals, this experimental pipeline allows the identification of reads that map to the HIV-1 genome.

Acknowledgments

We thank the HIV-1-positive individual who agreed to participate to the Seroconverter Study and provide his blood for research. We thank NIH AIDS Research & Reference Reagent Program for providing Vorinostat. This work was supported by funding of Berlin Institute of Health (BIH) to C.G. We thank Christian Drosten for constant support. J.K. is supported by the Center of Infection Biology and Immunity (ZIBI) and Charité PhD Program.

Author Contributions

J.K. and C.G. conceived and designed the experiments; J.K., J.J., S.N.V. and M.S. performed the experiments, J.K., D.P., E.W., C.F., K.M. and C.G. analyzed the data; J.K., D.P. and C.G. drafted the manuscript.; J.K., D.P. and C.G. wrote the manuscript.; S.S., N.B., M.L. and C.G. supervised the research.

Declaration of Interests

None

Legends

Figure 1. LRA treatment modulates CD4$^+$ T-subset composition

(**A**) UMAP plots of mock-, Vorinostat-, Panobinostat- and IL-2/PHA-treated CD4$^+$ T cells. The individual CD4$^+$ T-cell subsets are indicated by colouration.

(**B**) Pie charts indicating the relative percentage of individual CD4$^+$ T cell subset for indicated conditions.

(**C**) Raw counts and relative percentages of individual CD4$^+$ T cell subsets for indicated conditions.

Figure 2. LRA- and CD4$^+$ T-cell subset specific modulation of the transcriptome

(**A**) UMAP plots of the integrated analysis Vorinostat, Panobinostat and IL-2/PHA treated samples with the mock treated sample.

(**B**) Volcano plots of all significantly differentially regulated genes in each LRA treatment relative to the mock sample (minimum log e fold change of ±0.25, Bonferroni corrected p-value <0.05, Wilcoxon rank-sum test). Upregulated genes are indicated in red, downregulated genes in blue.

(**C**) Overlap in differentially regulated genes between treatments within each cell subset.

(**D**) Overlap of differentially regulated genes between cell subsets within each treatment.

(**E**) Pseudotime cell trajectory analysis and GSEA analysis using genes differentially regulated between the mock and Panobinostat treatments for T_N, T_{CM}, T_{TM} and T_{EM} cells, and for total CD4$^+$ T-cells. Cells are represented as arrayed along the Pseudotime trajectory, coloured by both treatment and their pseudotime scores.

(**F**) The top five most significantly positively and negatively enriched pathways (based on the associated p-value) for each cell subset are indicated, along with the corresponding normalised enrichment score (NES).

Figure 3. LRA treatment alters the expression of IRGs in CD4$^+$ T-cells in a treatment- and subset-specific manner

(**A**) Volcano plots of all significantly differentially regulated IRGs in each LRA treatment relative to the mock sample (minimum log e fold change of ±0.25, Bonferronni corrected p-value <0.05, Wilcoxon rank-sum test). Upregulated genes are indicated in red, downregulated genes in blue.

(**B**) Overlap of differentially regulated IRGs between cell subsets within each treatment.

(**C**) Overlap in differentially regulated IRGs between treatments within each cell subset.

(**D**) Heat maps indicating fold change in expression between mock and treated samples for selected IRGs with potential implications for anti-viral activity in the Vorinostat and Panobinostat treatments. The normalised fold change in IRG expression is shown (expression in mock treatment = 1). Crossed-out (X) fields represent genes that were not expressed in at least 10% of either the mock or treated sample. Average fold changes in gene expression for significantly differentially expressed IRGs are indicated above the corresponding violin plot for each cell type (Wilcoxon rank-sum test, Bonferroni corrected p-value <0.05).

(**E**) Violin plots showing normalised expression for selected IRGs with potential implications for anti-viral activity in the Vorinostat and Panobinostat treatments. Numbers indicate fold change expression of significantly deregulated IRGs.

References

Anderson, I., Low, J.S., Weston, S., Weinberger, M., Zhyvoloup, A., Labokha, A.A., Corazza, G., Kitson, R.A., Moody, C.J., Marcello, A., *et al.* (2014). Heat shock protein 90 controls HIV-1 reactivation from latency. Proc Natl Acad Sci U S A *111*, E1528-1537.

Archin, N.M., Liberty, A.L., Kashuba, A.D., Choudhary, S.K., Kuruc, J.D., Crooks, A.M., Parker, D.C., Anderson, E.M., Kearney, M.F., Strain, M.C., *et al.* (2012). Administration of vorinostat disrupts HIV-1 latency in patients on antiretroviral therapy. Nature *487*, 482-485.

Beliakova-Bethell, N., Mukim, A., White, C.H., Deshmukh, S., Abewe, H., Richman, D.D., and Spina, C.A. (2019). Histone deacetylase inhibitors induce complex host responses that contribute to differential potencies of these compounds in HIV reactivation. J Biol Chem *294*, 5576-5589.

Braun, E., Hotter, D., Koepke, L., Zech, F., Gross, R., Sparrer, K.M.J., Muller, J.A., Pfaller, C.K., Heusinger, E., Wombacher, R., *et al.* (2019). Guanylate-Binding Proteins 2 and 5 Exert Broad Antiviral Activity by Inhibiting Furin-Mediated Processing of Viral Envelope Proteins. Cell Rep *27*, 2092-2104 e2010.

Brinkmann, C.R., Hojen, J.F., Rasmussen, T.A., Kjaer, A.S., Olesen, R., Denton, P.W., Ostergaard, L., Ouyang, Z., Lichterfeld, M., Yu, X., *et al.* (2018). Treatment of HIV-Infected Individuals with the Histone Deacetylase Inhibitor Panobinostat Results in Increased Numbers of Regulatory T Cells and Limits Ex Vivo Lipopolysaccharide-Induced Inflammatory Responses. mSphere *3*.

Butler, A., Hoffman, P., Smibert, P., Papalexi, E., and Satija, R. (2018). Integrating single-cell transcriptomic data across different conditions, technologies, and species. Nat Biotechnol *36*, 411-420.

Chen, H. (2018). VennDiagram: Generate High-Resolution Venn and Euler Plots. R package version 1.6.20. https://CRANR-projectorg/package=VennDiagram.

Chomont, N., El-Far, M., Ancuta, P., Trautmann, L., Procopio, F.A., Yassine-Diab, B., Boucher, G., Boulassel, M.R., Ghattas, G., Brenchley, J.M., *et al.* (2009). HIV reservoir size and persistence are driven by T cell survival and homeostatic proliferation. Nat Med *15*, 893-900.

Cohn, L.B., da Silva, I.T., Valieris, R., Huang, A.S., Lorenzi, J.C.C., Cohen, Y.Z., Pai, J.A., Butler, A.L., Caskey, M., Jankovic, M., *et al.* (2018). Clonal CD4(+) T cells in the HIV-1 latent reservoir display a distinct gene profile upon reactivation. Nat Med *24*, 604-609.

Cohn, L.B., Silva, I.T., Oliveira, T.Y., Rosales, R.A., Parrish, E.H., Learn, G.H., Hahn, B.H., Czartoski, J.L., McElrath, M.J., Lehmann, C., *et al.* (2015). HIV-1 integration landscape during latent and active infection. Cell *160*, 420-432.

Compton, A.A., Bruel, T., Porrot, F., Mallet, A., Sachse, M., Euvrard, M., Liang, C., Casartelli, N., and Schwartz, O. (2014). IFITM proteins incorporated into HIV-1 virions impair viral fusion and spread. Cell Host Microbe *16*, 736-747.

Dusa, A. (2020). venn: Draw Venn Diagrams. R package version 1.9. https://CRANR-projectorg/package=venn.

Finzi, D., Blankson, J., Siliciano, J.D., Margolick, J.B., Chadwick, K., Pierson, T., Smith, K., Lisziewicz, J., Lori, F., Flexner, C., *et al.* (1999). Latent infection of CD4+ T cells provides a mechanism for lifelong persistence of HIV-1, even in patients on effective combination therapy. Nat Med *5*, 512-517.

Foster, T.L., Wilson, H., Iyer, S.S., Coss, K., Doores, K., Smith, S., Kellam, P., Finzi, A., Borrow, P., Hahn, B.H., *et al.* (2016). Resistance of Transmitted Founder HIV-1 to IFITM-Mediated Restriction. Cell Host Microbe *20*, 429-442.

Golubovskaya, V., and Wu, L. (2016). Different Subsets of T Cells, Memory, Effector Functions, and CAR-T Immunotherapy. Cancers (Basel) *8*.

Goujon, C., Moncorge, O., Bauby, H., Doyle, T., Ward, C.C., Schaller, T., Hue, S., Barclay, W.S., Schulz, R., and Malim, M.H. (2013). Human MX2 is an interferon-induced post-entry inhibitor of HIV-1 infection. Nature *502*, 559-562.

Govindaraj, C., Tan, P., Walker, P., Wei, A., Spencer, A., and Plebanski, M. (2014). Reducing TNF receptor 2+ regulatory T cells via the combined action of azacitidine and the HDAC inhibitor, panobinostat for clinical benefit in acute myeloid leukemia patients. Clin Cancer Res *20*, 724-735.

Grau-Exposito, J., Luque-Ballesteros, L., Navarro, J., Curran, A., Burgos, J., Ribera, E., Torrella, A., Planas, B., Badia, R., Martin-Castillo, M., *et al.* (2019). Latency reversal agents affect differently the latent reservoir present in distinct CD4+ T subpopulations. PLoS Pathog *15*, e1007991.

Han, X., Wei, Y., Wang, H., Wang, F., Ju, Z., and Li, T. (2018). Nonsense-mediated mRNA decay: a 'nonsense' pathway makes sense in stem cell biology. Nucleic Acids Res *46*, 1038-1051.

Hrecka, K., Hao, C., Gierszewska, M., Swanson, S.K., Kesik-Brodacka, M., Srivastava, S., Florens, L., Washburn, M.P., and Skowronski, J. (2011). Vpx relieves inhibition of HIV-1 infection of macrophages mediated by the SAMHD1 protein. Nature *474*, 658-661.

Hurst, J., Hoffmann, M., Pace, M., Williams, J.P., Thornhill, J., Hamlyn, E., Meyerowitz, J., Willberg, C., Koelsch, K.K., Robinson, N., *et al.* (2015). Immunological biomarkers predict HIV-1 viral rebound after treatment interruption. Nat Commun *6*, 8495.

Jassal, B., Matthews, L., Viteri, G., Gong, C., Lorente, P., Fabregat, A., Sidiropoulos, K., Cook, J., Gillespie, M., Haw, R., *et al.* (2020). The reactome pathway knowledgebase. Nucleic Acids Res *48*, D498-D503.

Jonsson, K.L., Tolstrup, M., Vad-Nielsen, J., Kjaer, K., Laustsen, A., Andersen, M.N., Rasmussen, T.A., Sogaard, O.S., Ostergaard, L., Denton, P.W., *et al.* (2015). Histone deacetylase inhibitor romidepsin inhibits de novo HIV-1 infections. Antimicrob Agents Chemother *59*, 3984-3994.

Kane, M., Yadav, S.S., Bitzegeio, J., Kutluay, S.B., Zang, T., Wilson, S.J., Schoggins, J.W., Rice, C.M., Yamashita, M., Hatziioannou, T., *et al.* (2013). MX2 is an interferon-induced inhibitor of HIV-1 infection. Nature *502*, 563-566.

Kim, Y., Anderson, J.L., and Lewin, S.R. (2018). Getting the "Kill" into "Shock and Kill": Strategies to Eliminate Latent HIV. Cell Host Microbe *23*, 14-26.

Korotkevich, G., Sukhov, V., and Sergushichev, A. (2019). Fast gene set enrichment analysis. biorxiv doi: 101101/060012.

Krapp, C., Hotter, D., Gawanbacht, A., McLaren, P.J., Kluge, S.F., Sturzel, C.M., Mack, K., Reith, E., Engelhart, S., Ciuffi, A., *et al.* (2016). Guanylate Binding Protein (GBP) 5 Is an Interferon-Inducible Inhibitor of HIV-1 Infectivity. Cell Host Microbe *19*, 504-514.

Laguette, N., Sobhian, B., Casartelli, N., Ringeard, M., Chable-Bessia, C., Segeral, E., Yatim, A., Emiliani, S., Schwartz, O., and Benkirane, M. (2011). SAMHD1 is the dendritic- and myeloid-cell-specific HIV-1 restriction factor counteracted by Vpx. Nature *474*, 654-657.

Liu, Z., Pan, Q., Ding, S., Qian, J., Xu, F., Zhou, J., Cen, S., Guo, F., and Liang, C. (2013). The interferon-inducible MxB protein inhibits HIV-1 infection. Cell Host Microbe *14*, 398-410.

Lucera, M.B., Tilton, C.A., Mao, H., Dobrowolski, C., Tabler, C.O., Haqqani, A.A., Karn, J., and Tilton, J.C. (2014). The histone deacetylase inhibitor vorinostat (SAHA) increases the susceptibility of uninfected CD4+ T cells to HIV by increasing the kinetics and efficiency of postentry viral events. J Virol *88*, 10803-10812.

Machnowska, P., Meixenberger, K., Schmidt, D., Jessen, H., Hillenbrand, H., Gunsenheimer-Bartmeyer, B., Hamouda, O., Kucherer, C., Bannert, N., and German, H.I.V.S.S.G. (2019). Prevalence and persistence of transmitted drug resistance mutations in the German HIV-1 Seroconverter Study Cohort. PLoS One *14*, e0209605.

MacLeod, M.K., Clambey, E.T., Kappler, J.W., and Marrack, P. (2009). CD4 memory T cells: what are they and what can they do? Semin Immunol *21*, 53-61.

Mahnke, Y.D., Brodie, T.M., Sallusto, F., Roederer, M., and Lugli, E. (2013). The who's who of T-cell differentiation: human memory T-cell subsets. Eur J Immunol *43*, 2797-2809.

Margolis, D.M., Garcia, J.V., Hazuda, D.J., and Haynes, B.F. (2016). Latency reversal and viral clearance to cure HIV-1. Science *353*, aaf6517.

Mercier, S., St-Pierre, C., Pelletier, I., Ouellet, M., Tremblay, M.J., and Sato, S. (2008). Galectin-1 promotes HIV-1 infectivity in macrophages through stabilization of viral adsorption. Virology *371*, 121-129.

Olesen, R., Vigano, S., Rasmussen, T.A., Sogaard, O.S., Ouyang, Z., Buzon, M., Bashirova, A., Carrington, M., Palmer, S., Brinkmann, C.R., *et al.* (2015). Innate Immune Activity Correlates with CD4 T Cell-Associated HIV-1 DNA Decline during Latency-Reversing Treatment with Panobinostat. J Virol *89*, 10176-10189.

Ouellet, M., Mercier, S., Pelletier, I., Bounou, S., Roy, J., Hirabayashi, J., Sato, S., and Tremblay, M.J. (2005). Galectin-1 acts as a soluble host factor that promotes HIV-1 infectivity through stabilization of virus attachment to host cells. J Immunol *174*, 4120-4126.

Rasmussen, T.A., Schmeltz Sogaard, O., Brinkmann, C., Wightman, F., Lewin, S.R., Melchjorsen, J., Dinarello, C., Ostergaard, L., and Tolstrup, M. (2013). Comparison of HDAC inhibitors in clinical development: effect on HIV production in latently infected cells and T-cell activation. Hum Vaccin Immunother *9*, 993-1001.

Rasmussen, T.A., Tolstrup, M., Brinkmann, C.R., Olesen, R., Erikstrup, C., Solomon, A., Winckelmann, A., Palmer, S., Dinarello, C., Buzon, M., *et al.* (2014). Panobinostat, a histone

deacetylase inhibitor, for latent-virus reactivation in HIV-infected patients on suppressive antiretroviral therapy: a phase 1/2, single group, clinical trial. Lancet HIV *1*, e13-21.

Ross, S.H., and Cantrell, D.A. (2018). Signaling and Function of Interleukin-2 in T Lymphocytes. Annu Rev Immunol *36*, 411-433.

Rusinova, I., Forster, S., Yu, S., Kannan, A., Masse, M., Cumming, H., Chapman, R., and Hertzog, P.J. (2013). Interferome v2.0: an updated database of annotated interferon-regulated genes. Nucleic Acids Res *41*, D1040-1046.

Sanchez, I., and Dynlacht, B.D. (2016). Cilium assembly and disassembly. Nat Cell Biol *18*, 711-717.

Sheehy, A.M., Gaddis, N.C., Choi, J.D., and Malim, M.H. (2002). Isolation of a human gene that inhibits HIV-1 infection and is suppressed by the viral Vif protein. Nature *418*, 646-650.

Siliciano, J.D., Kajdas, J., Finzi, D., Quinn, T.C., Chadwick, K., Margolick, J.B., Kovacs, C., Gange, S.J., and Siliciano, R.F. (2003). Long-term follow-up studies confirm the stability of the latent reservoir for HIV-1 in resting CD4+ T cells. Nat Med *9*, 727-728.

Sogaard, O.S., Graversen, M.E., Leth, S., Olesen, R., Brinkmann, C.R., Nissen, S.K., Kjaer, A.S., Schleimann, M.H., Denton, P.W., Hey-Cunningham, W.J., *et al.* (2015). The Depsipeptide Romidepsin Reverses HIV-1 Latency In Vivo. PLoS Pathog *11*, e1005142.

St-Pierre, C., Manya, H., Ouellet, M., Clark, G.F., Endo, T., Tremblay, M.J., and Sato, S. (2011). Host-soluble galectin-1 promotes HIV-1 replication through a direct interaction with glycans of viral gp120 and host CD4. J Virol *85*, 11742-11751.

Tartour, K., Appourchaux, R., Gaillard, J., Nguyen, X.N., Durand, S., Turpin, J., Beaumont, E., Roch, E., Berger, G., Mahieux, R., *et al.* (2014). IFITM proteins are incorporated onto HIV-1 virion particles and negatively imprint their infectivity. Retrovirology *11*, 103.

R Core Team, (2017). R: A language and environment for statistical computing. R Foundation for Statistical Computing, Vienna, Austria; https://wwwR-projectorg/.

Trapnell, C., Cacchiarelli, D., Grimsby, J., Pokharel, P., Li, S., Morse, M., Lennon, N.J., Livak, K.J., Mikkelsen, T.S., and Rinn, J.L. (2014). The dynamics and regulators of cell fate decisions are revealed by pseudotemporal ordering of single cells. Nat Biotechnol *32*, 381-386.

Tsai, P., Wu, G., Baker, C.E., Thayer, W.O., Spagnuolo, R.A., Sanchez, R., Barrett, S., Howell, B., Margolis, D., Hazuda, D.J., *et al.* (2016). In vivo analysis of the effect of panobinostat on cell-associated HIV RNA and DNA levels and latent HIV infection. Retrovirology *13*, 36.

Vanhamel, J., Bruggemans, A., and Debyser, Z. (2019). Establishment of latent HIV-1 reservoirs: what do we really know? J Virus Erad *5*, 3-9.

von Stockenstrom, S., Odevall, L., Lee, E., Sinclair, E., Bacchetti, P., Killian, M., Epling, L., Shao, W., Hoh, R., Ho, T., *et al.* (2015). Longitudinal Genetic Characterization Reveals That Cell Proliferation Maintains a Persistent HIV Type 1 DNA Pool During Effective HIV Therapy. J Infect Dis *212*, 596-607.

Wagner, T.A., McLaughlin, S., Garg, K., Cheung, C.Y., Larsen, B.B., Styrchak, S., Huang, H.C., Edlefsen, P.T., Mullins, J.I., and Frenkel, L.M. (2014). HIV latency. Proliferation of

cells with HIV integrated into cancer genes contributes to persistent infection. Science *345*, 570-573.

Wang, S., Zhang, Q., Hui, H., Agrawal, K., Karris, M.A.Y., and Rana, T. (2019). An Atlas of Immune Cell Exhaustion in HIV-Infected Individuals Revealed by Single-Cell Transcriptomics. bioRxiv doi: 101101/678763.

Weatherly, K., Bettonville, M., Torres, D., Kohler, A., Goriely, S., and Braun, M.Y. (2015). Functional profile of S100A4-deficient T cells. Immun Inflamm Dis *3*, 431-444.

White, C.H., Beliakova-Bethell, N., Lada, S.M., Breen, M.S., Hurst, T.P., Spina, C.A., Richman, D.D., Frater, J., Magiorkinis, G., and Woelk, C.H. (2018). Transcriptional Modulation of Human Endogenous Retroviruses in Primary CD4+ T Cells Following Vorinostat Treatment. Front Immunol *9*, 603.

Kazmierski *et al.*, Figure 1

A

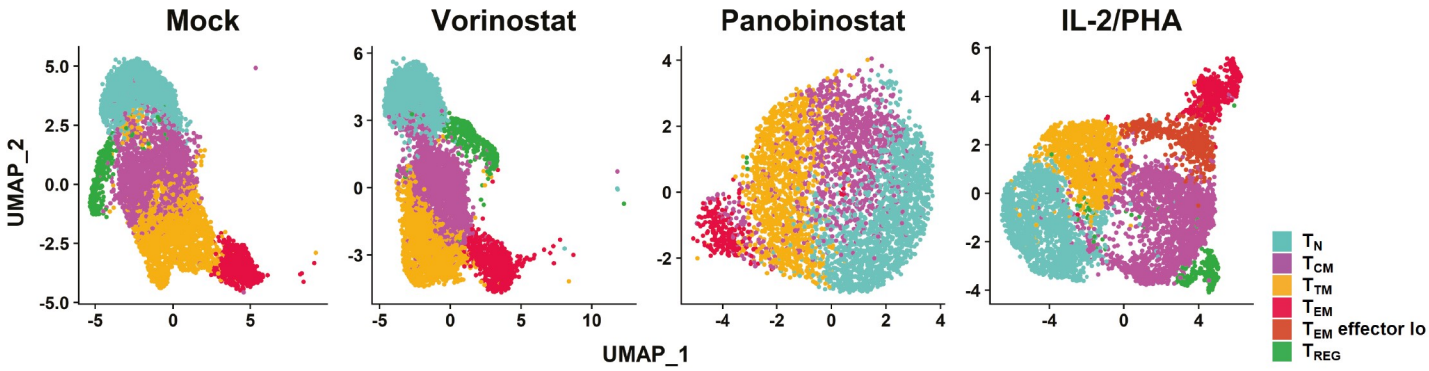

B

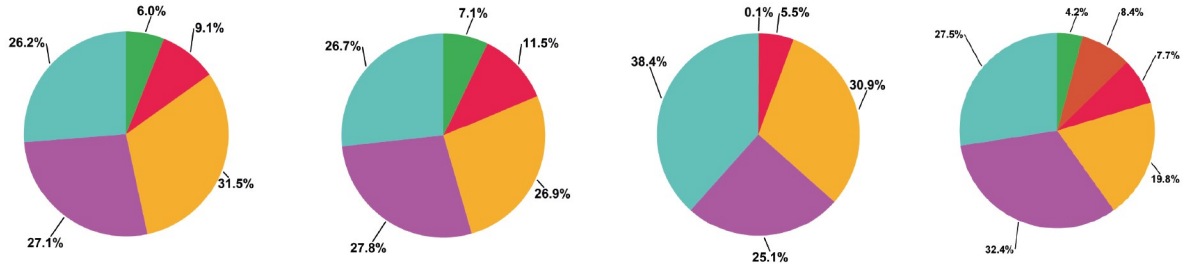

C

Treatment	Mock		Vorinostat		Panobinostat		IL-2/PHA	
	counts	ratio	counts	ratio	counts	ratio	counts	ratio
T_N	1544	26.2%	1815	26.7%	1854	31.5%	1607	27.5
T_{CM}	1594	27.1%	1885	27.8%	1824	26.9%	1895	32.4%
T_{TM}	1854	31.5%	1824	26.9%	1295	30.9%	1158	19.8%
T_{EM}	535	9.1%	782	11.5%	1158	19.8%	450	7.7%
T_{EM} effector lo	0	0%	0	0%	0	0%	493	8.4%
T_{REG}	355	6.0%	484	7.1%	4	0.1%	247	4.2%
Total counts	5882		6790		4193		5850	

Kazmierski *et al.*, Figure 2

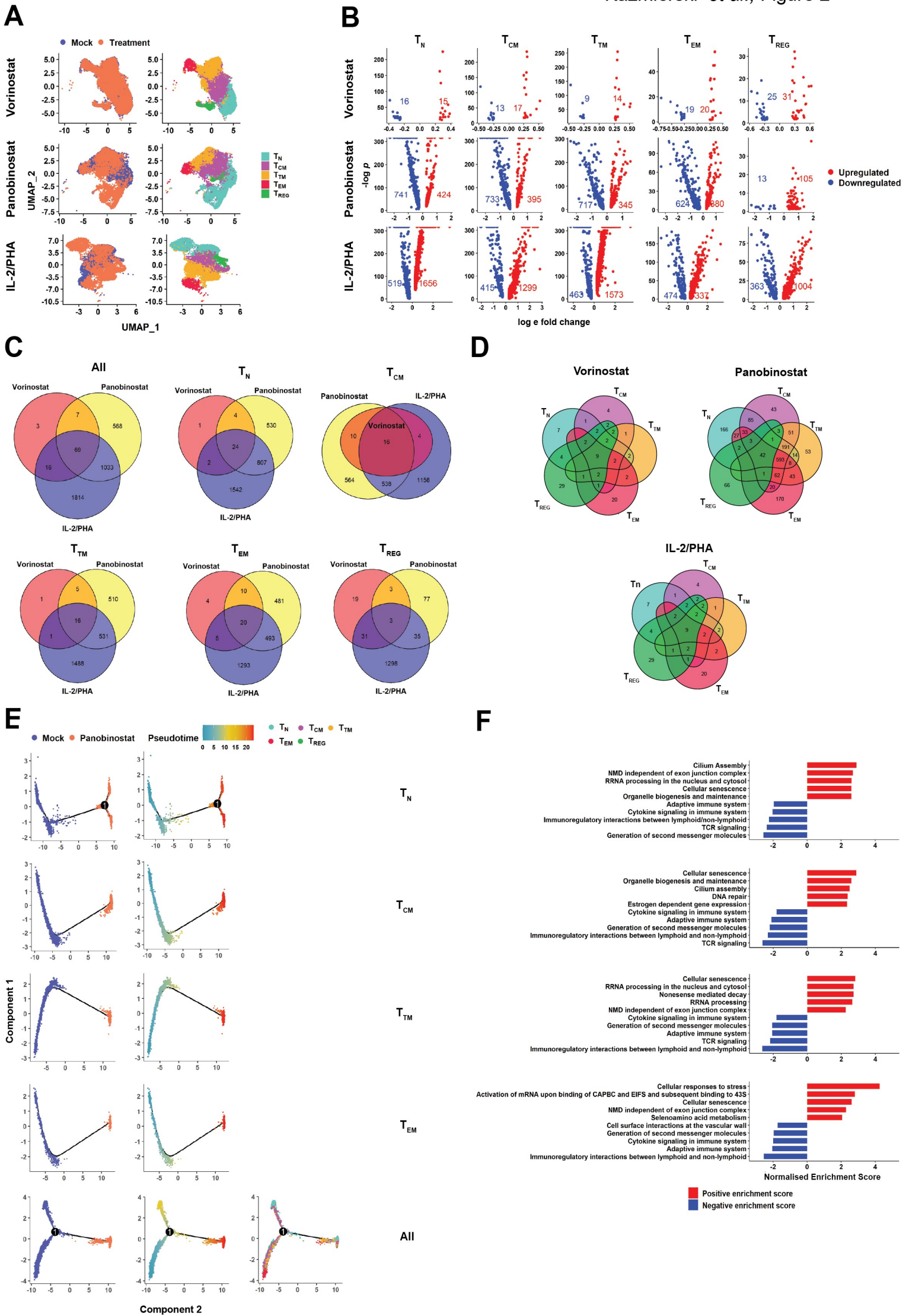

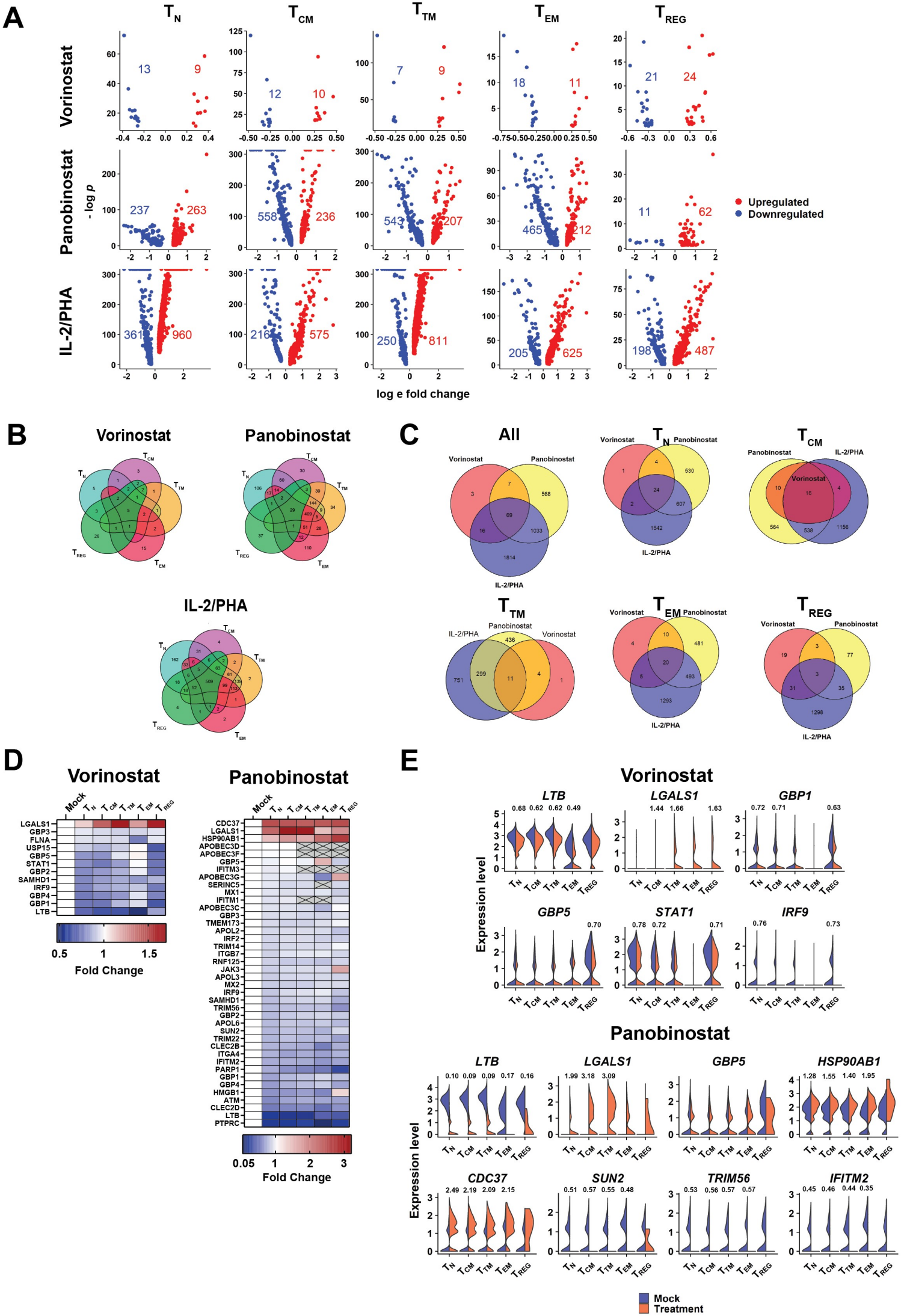
A
T_N
T_CM
T_TM
T_EM
T_REG
Vorinostat
Panobinostat
IL-2/PHA
- log p
log e fold change
Upregulated
Downregulated
B
Vorinostat
Panobinostat
IL-2/PHA
C
All
Vorinostat
Panobinostat
IL-2/PHA
D
Vorinostat
Panobinostat
Mock
LGALS1
GBP3
FLNA
USP15
GBP5
STAT1
GBP2
SAMHD1
IRF9
GBP4
GBP1
LTB
Fold Change
CDC37
HSP90AB1
APOBEC3D
APOBEC3F
IFITM3
APOBEC3G
SERINC5
MX1
IFITM1
APOBEC3C
TMEM173
APOL2
IRF2
TRIM14
ITGB7
RNF125
JAK3
APOL3
MX2
TRIM56
APOL6
SUN2
TRIM22
CLEC2B
ITGA4
IFITM2
PARP1
HMGB1
ATM
CLEC2D
PTPRC
E
Vorinostat
Panobinostat
Expression level
LTB
LGALS1
GBP1
GBP5
STAT1
IRF9
HSP90AB1
CDC37
SUN2
TRIM56
IFITM2
Mock
Treatment